ELSEVIER

1 August 1997

Chemical Physics Letters 274 (1997) 58–62

CHEMICAL PHYSICS LETTERS

Time-resolved FTIR study of the 308 nm photolysis of NO_2. Nascent vibrational populations and quenching of NO($v = 1-3$)

Alan Doughty, Gus Hancock, Emily L. Moore

Physical and Theoretical Chemistry Laboratory, Oxford University, South Parks Rd., Oxford OX1 3QZ, UK

Received 22 April 1997; in final form 28 May 1997

Abstract

The nascent distribution of the vibrationally excited NO product of NO_2 photolysis at 308 nm has been determined by time-resolved FTIR spectroscopy. The percentage distribution in the excited vibrational levels $v = 1{:}2{:}3$ was found to be $(28 \pm 3{:}38 \pm 4{:}34 \pm 4)$, with negligible population in higher levels. The distribution is inconsistent with that predicted from simple statistical theories, and indicates that at this wavelength dynamical effects control the vibrational energy partitioning. The quenching of NO(v) by NO_2 is dominated by single quantum energy transfer, but does not populate the closely resonant (0, 0, 1) level of NO_2 with unit efficiency. © 1997 Elsevier Science B.V.

1. Introduction

The energy distributions in the products of the photolysis of NO_2 have long been used to infer details of the photodissociation dynamics, particularly because of the ease by which the NO product in its ground $^2\Pi$ state can be detected by laser-induced fluorescence (LIF). Although LIF can provide unprecedented detail about the relative rotational, spin orbit and lambda doublet populations in a given NO vibrational state, it is less straightforward to use for the determination of vibrational population distributions. This is because LIF signals which probe different vibrational levels necessarily involve changes in either or both of the absorption and emission wavelengths, and careful corrections need to be made for the transition probabilities of the probed bands, and for the wavelength dependences of the excitation and detection systems.

Observation of IR emission from vibrationally excited levels offers a complementary way of studying the vibrational populations. Although this method has the disadvantages that it cannot match LIF in sensitivity, and it provides no information on the ground vibrational state, its advantage is that all emitting species can be observed simultaneously, and the signals require straightforward conversion to relative populations. Here we describe the use of a time-resolved Fourier transform infrared emission (FTIR) technique to measure the nascent vibrational distribution of NO($v = 1-3$) from the dissociation of NO_2 at 308 nm. There are two previously reported studies of vibrational populations in this wavelength region, both carried out by LIF. Zacharias et al. [1] found the percentage distribution for photolysis of a room temperature sample at 308 nm to be $v = 0{:}1{:}2{:}3{:}4 = 29{:}28{:}19{:}21.5{:}2.5$, i.e., with little marked variation in the first four levels. Knepp et al. [2] photolysed a jet cooled (< 10 K) sample at 309.1 nm, and found a monotonically decreasing population, with $v = 0{:}1{:}2{:}3 = 44{:}28{:}16{:}12$. Knepp et al. [2] argue that their results show that the vibrational

0009-2614/97/$17.00
PII S0009-2614(97)00645-3

partitioning is closer to being statistical, as seen for photolysis near threshold [3,4], than to being controlled by the dynamical effects which result in the population inversion in higher vibrational levels seen for photolysis at 248 nm [5,6]. Our observations of the time-resolved emission from NO are closer in agreement with the non-statistical observations of Zacharias et al. [1] and are also able to demonstrate some details of the fate of the excitation collisionally transferred from these vibrationally excited levels.

2. Experimental

Radiation at 308 nm from a XeCl excimer laser (Lambda Physik LPX110i) was multipassed through a photolysis cell fitted with Welsh collection optics. The IR fluorescence was passed into a Michelsen interferometer operating in step-scan mode as described previously [7]. The signal was detected with a liquid nitrogen cooled HgCdTe device, which, together with its associated amplifier, had a rise time of 3.4 μs. Data were taken with a spectral resolution of 16 cm^{-1} and a temporal resolution of 2 μs.

Measurements of the contribution of NO($v = 1$–0) emission to the total NO signal were made with a cold gas filter, 9 cm long and filled with 0.1 to 40 Torr NO, placed in the pathway of the emitted IR radiation. An additional optical filter allowing the transmission of the $\Delta v = -1$ bands of NO($v = 1$–3) between 1700–2500 cm^{-1} was also placed in the path of the emission signal. Comparison of the emission intensity for a known pressure of NO in the cold gas filter with that for an empty cell allowed the proportion of radiation arising from NO($v = 1$) and passing through the interference filter to be calculated. Care was taken to ensure that only emission from NO($v = 1$) was absorbed, and that non-resonant absorption was not significant.

NO_2 (BOC, > 99.5%) was purified by reaction with oxygen (BOC, > 99.5%) in excess of the NO impurity level. The oxygen was then removed by freeze–pump–thaw cycles at dry ice temperatures. NO (MG Gases, > 99.5%) was purified by passing it slowly over a cold trap maintained at dry ice temperature at pressures below 10 Torr. Argon (BOC, > 99.99%) and NO_2 pressures in the photolysis vessel were controlled by setting the gas flows (by means of Tylan mass flow controllers and ball flow meters respectively), and the photolysis vessel pumping speed. All experiments were carried out at room temperature, 295 K.

3. Results

Experiments were carried out at a range of NO_2 pressures from 50 to 500 mTorr in 5 Torr of argon, and at a constant pressure of 100 mTorr NO_2 in argon pressures ranging from 1 to 10 Torr. Fig. 1 shows an example of the time-resolved spectra, indicating two regions of emission near 1800 and 1600 cm^{-1}. The former peak appeared promptly after the photolysis laser pulse, with the emission rising rate corresponding to the instrument response time of 3.4 μs, and is seen to decay and shift to higher wavenumbers at longer times. The emission is identified as the $\Delta v = -1$ bands of NO, changing intensity and wavenumber as a consequence of vibrational quenching. It is the change in shape of the NO emission that forms the basis for extracting the time dependent vibrational populations in this study. The feature near 1600 cm^{-1} was identified as the (0, 0, 1)–(0, 0, 0) band of NO_2 (which has its band origin

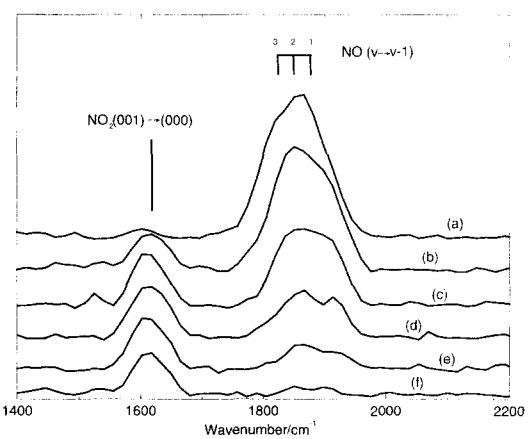

Fig. 1. Time-resolved spectra from the 308 nm photolysis of NO_2 (0.253 Torr) in Ar (5.1 Torr). Traces (a)–(f) were taken at increasing times of 20, 44, 74, 104, 134 and 194 μs after photolysis, and are averaged over 8 μs intervals. Prompt emission between 1800–1900 cm^{-1} is attributed to NO($v \rightarrow v - 1$) and the band origins for $v = 1$–3 are shown in the Figure. Emission near 1618 cm^{-1} is from the NO_2 (0, 0, 1)→(0, 0, 0) transition. Spectral resolution 16 cm^{-1}.

at 1618 cm^{-1} and which was confirmed by cold gas filter experiments), and its appearance at later times indicates that it is formed by an energy transfer process. The rate of loss of the total NO signal was approximately equal to the rate of rise of the NO_2 signal.

Synthetic spectra were generated for the NO $\Delta v = -1$ bands, $v = 1$–4, from published spectral data [8] and Einstein A-coefficients [9], with an assumed rotational temperature of 300 K, and with corrections for instrumental response and resolution. Previous measurements of NO rotational relaxation following the photolysis of NO_2 at 308 nm have shown that collapse of the nascent rotationally excited distribution to a room temperature Boltzmann distribution in collisions with Ar would take place by the earliest times at which data were taken in the present experiments [10]. An iterative least squares fitting procedure [11] was used to fit the synthetic spectra to the experimental data, with the relative populations of NO($v = 1$–4) as variables. Examples of the fits with contributions from $v = 1$–3 are shown in Fig. 2. No contribution from NO($v \geq 4$) was observed.

The spectral fitting procedure was carried out at 2-μs intervals after the photolysis pulse for each of the emission spectra, and an example is shown of the resultant time evolution of the NO vibrational populations in Fig. 3. As can be seen from the Figure, the instrument rise time prevents the nascent vibrational

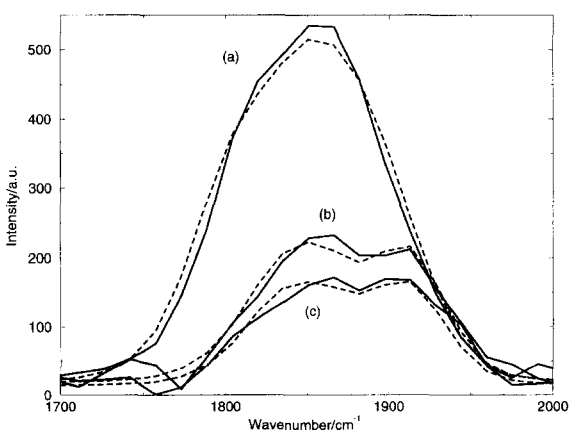

Fig. 2. Experimental spectra near 1800 cm^{-1} (solid lines) compared with fitted spectra (dashed lines). Traces (a), (b) and (c) were taken at 11, 81 and 101 μs after photolysis at 2 μs resolution. Other conditions as for Fig. 1.

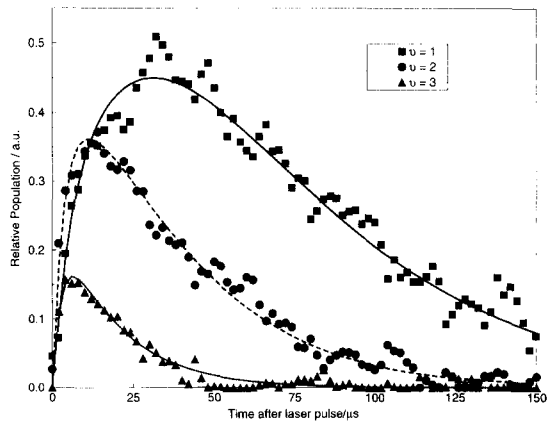

Fig. 3. Time-resolved populations of NO $v = 1$ (■), $v = 2$ (●) and $v = 3$ (▲) obtained from fits such as those shown in Fig. 2, from data at 2 μs intervals. The lines show the fits to the data from the model explained in the text.

populations being determined directly by spectral fitting. What however is clear is that the highest vibrational level ($v = 3$) has the fastest rise, and the lowest, $v = 1$, peaks at a time which is considerably after the laser pulse and which was found to decrease as the pressure of NO_2 was raised. In order to obtain the nascent vibrational distribution the evolution of the temporal profiles of the NO(v) populations were modelled in the following way. Six adjustable parameters were used to fit each of the 13 sets of experimental data at different pressures of NO_2 and Ar, namely the initial populations in $v = 1$–3 from 308 nm photolysis, and the quenching rates out of these levels in collisions with NO_2 (the effect of quenching by Ar was found to be negligible). The quenching processes were assumed to be dominated by single quantum loss processes in NO:

$$\mathrm{NO}(v) + \mathrm{NO_2}(0,0,0) \rightarrow \mathrm{NO}(v-1) + \mathrm{NO_2}(l,m,n). \quad (1)$$

Such processes were found necessary to explain the rise of population in lower levels, particularly in $v = 1$, seen under all conditions after photolysis. Inclusion of processes in which all initial quanta in NO are lost in collisions with NO_2, such as might be expected for the formation of a long lived complex in which energy is fully randomised, gave unacceptable fits to levels other than $v = 3$.

Vibrationally excited NO is also formed in the secondary reaction

$$O(^3P) + NO_2 \rightarrow O_2 + NO, \quad (2)$$

where O atoms are produced in the 308 nm photolysis step, and was included in the fitting procedure. The nascent NO population in this reaction peaks at $v = 0$, with percentage yields in $v = 1$ and 2 of 17 ± 7 and 3 ± 1.5 respectively [12]. The contribution from this reaction was determined by an iterative procedure, where the $O(^3P)$ concentration was taken as the sum of $NO(v = 0–3)$ formed by photolysis, with the unmeasured $NO(v = 0)$ determined using a surprisal plot of the initial $NO(v = 1–3)$ populations. To assess the magnitude of the error that this could introduce into the determination of populations, particularly in $v = 1$, simulations were carried out with $NO(v = 0)$ set to 0, and also to the sum of $NO(v = 1–3)$. These can be considered as minimum and maximum possible values for the nascent $NO(v = 0)$ photolytic populations. Populations of $NO(v = 1)$ obtained in this way showed only a small dependence on the $NO(v = 0)$ estimate used, and the range of values were found to fall within the errors limits of the nascent populations averaged over all the experimental runs.

Fig. 3 shows one example of the fits to the experimental data. The nascent distributions were found to be invariant with the range of NO_2 and Ar pressures studied, consistent with the assumption of rotational relaxation within the system. Mean values of the 13 sets of data weighted according to the error ranges returned from the fitting routines are given in Table 1. The quenching rates increased linearly with NO_2 pressure, and the rate constants showed an increase with NO vibrational quantum number, with that for $v = 1$, $(1.9 \pm 0.2) \times 10^{-12}$ $cm^3 molecule^{-1} s^{-1}$ in excellent agreement with previously reported values [13,14]. These and other rate constants for energy transfer in this system will be described in a future publication [15].

Table 1
Nascent populations in NO ($v = 1–4$) from the photolysis of NO_2 near 308 nm. The results have been normalised to 100 for $v = 1–4$

	$v = 1$	$v = 2$	$v = 3$	$v = 4$
present results	28 ± 3	38 ± 4	34 ± 4	
Zacharias et al. [1]	39 ± 4	27 ± 2	30 ± 3	4 ± 0.4
Knepp et al. [2]	50 ± 8	29 ± 8	21 ± 12	

Cold gas filter experiments were carried out for photolysis of NO_2 at pressures ranging from 50–275 mTorr, with added gases (in this case either Ar or O_2) ranging from 1 to 10 Torr. The percentage p of emission from $NO(v = 1)$ which passes through the interference filter increased monotonically to a long time value of 100%, and was extrapolated smoothly to time zero. Care was taken to ensure that the detector risetime and contributions from reaction (2) were not distorting the extrapolations. The average of 9 separate experiments at different NO_2 pressures yielded a zero time value of $p = 25 \pm 4\%$, with the lack of a systematic total pressure dependence again showing the results are consistent with rotational relaxation of the nascent $NO(v = 1)$ having taken place.

4. Discussion

Table 1 compares our results with those previously measured. We observe a mildly inverted population between $v = 1$ and $v = 2$ and equal populations, within experimental error in $v = 2$ and 3. This result is in reasonable agreement with that of Zacharias et al. [1] but less so with the more recent results of Knepp et al. [2]. The percentage of emission from $v = 1$ that we would expect to see in the cold gas filter experiments can be calculated from the three distributions of Table 1 as 20 ± 2 (present results), 30 ± 3 [1] and $39 \pm 7\%$ [2], in comparison with our experimental value of $25 \pm 4\%$. This result is just equal within experimental error to that predicted from our vibrational state distribution obtained from the spectral analysis and to that calculated from the results of Zacharias et al. [1], but again is inconsistent with the colder vibrational distribution observed by Knepp et al. [2]. The latter results were explained as being consistent with straightforward statistical theories of energy partitioning such as phase space theory, which would predict a vibrational population which decreases monotonically with increasing v [2]. The present data clearly do not agree with this explanation, but

are more consistent with a modified statistical approach, the separate statistical ensemble (SSE) theory, which allows for some dynamical constraints [16]. If product vibration is allowed to evolve purely from parent vibrational degrees of freedom, and if the vibrational bending mode is treated as an internal rotor, then SSE theory predicts an equal population in each vibrational level in NO [2,4], and thus produces results which are close to being compatible with our present data and those of Zacharias et al. [1] (although failing to account for the population inversion that we see between $v = 1$ and 2). We conclude that at this wavelength the dissociation is either controlled dynamically (as appears to be the case at 248 nm [6]), or that statistical theories with some dynamical constraints such as SSE are required to explain the data.

Fig. 1 shows that $NO_2(0, 0, 1)$ is formed in the experiment, and the observation that its rising rate is approximately equal to the falling rate of the whole NO emission would at first sight suggest direct formation by process (1) with $(l, m, n) = (0, 0, 1)$, which is 258 cm^{-1} exothermic for $v = 1$, and becomes closer into resonance for higher v. Although the kinetics of the rising rate are compatible with this formation scheme of $NO_2(0, 0, 1)$ (which has been suggested to explain the relatively fast relaxation rate of $NO(v = 1)$ by NO_2 [13]), the relative intensities of the emission bands from NO and NO_2 are not. The Einstein emission coefficient for the $NO_2(0, 0, 1)$–$(0, 0, 0)$ band is almost an order of magnitude larger than that for $NO(v = 1–0)$. A reaction scheme which considers only energy transfer by process (1) followed by slower relaxation of NO_2 would predict a maximum signal at 1600 cm^{-1} which is far larger than that from NO at 1800 cm^{-1}, the reverse of what is observed in Fig. 1 (self absorption by NO_2 in the Welsh cell will alter the relative peak heights, but not by enough to invalidate this conclusion). Experiments at different excitation wavelengths have shown that the dominant route for $NO_2(0, 0, 1)$ excitation under these conditions is the relatively slow transfer from O_2 formed with considerable vibrational excitation in process (2) [15], and that the rise of the $NO_2(0, 0, 1)$ signal is kinetically controlled by the faster rate of quenching by ground state NO_2. Although single quantum loss dominates the fate of vibrationally excited NO, this leads to transfer to the energetically closest state, (0, 0, 1), in NO_2 with less than unit efficiency [15]. These measurements illustrate the advantages of using the IR emission technique to observe both donor and potential acceptor levels in vibrational energy transfer.

Acknowledgements

We are grateful to the NERC for support of this work. ELM thanks the Rhodes Trust for the award of a Scholarship.

References

[1] H. Zacharias, K. Meier and K.H. Welge, in: Energy Storage and Redistribution in Molecules, ed. J. Hinze (Plenum, New York, 1983) p. 107.
[2] P.T. Knepp, A.C. Terentis, S.H. Kable, J. Chem. Phys. 103 (1995) 195.
[3] D.C. Robie, M. Hunter, J.L. Bates, H. Reisler, Chem. Phys. Lett. 193 (1992) 413.
[4] M. Hunter, S.A. Reid, D.C. Robie, H. Reisler, J. Chem. Phys. 99 (1993) 1093.
[5] T.G. Slanger, W.K. Bischel, M.J. Dyer, J. Chem. Phys. 79 (1983) 2231.
[6] J. McFarlane, J.C. Polanyi, J.G. Shapter, J. Photochem. Photobiol. A 58 (1991) 139.
[7] P. Biggs, G. Hancock, D.E. Heard, R.P. Wayne, Meas. Sci. Technol. 1 (1990) 630.
[8] K.P. Huber and G. Herzberg, Molecular Spectra and Molecular Structure IV: Constants of Diatomic Molecules (Van Nostrand Reinhold, New York, 1979).
[9] S.R. Langhoff, Chem. Phys. Lett. 223 (1994) 416.
[10] U. Robra, Ph.D. Thesis, Universität Bielefeld (1984).
[11] W.H. Press, P.B. Flannery, S.A. Tenkolsky and W.T. Vetterling, Numerical Recipes. The Art of Scientific Computing, (Cambridge University Press, Cambridge, 1986).
[12] I.W.M. Smith, R.P. Tuckett, C.J. Whitham, Chem. Phys. Lett. 200 (1992) 615.
[13] J.C. Stephenson, J. Chem. Phys. 59 (1973) 1523.
[14] R.P. Fernando and I.W.M. Smith, J. Chem. Soc. Faraday Trans. 277 (1981) 459.
[15] G. Hancock and E.L. Moore, to be published.
[16] C. Wittig, I. Nadler, H. Reisler, M. Noble, J. Catanzarite, G. Radhakrishnan, J. Chem. Phys. 83 (1985) 5581.